DTU Library

Estimation of pulses in ultrasound B-scan images

Jensen, Jørgen Arendt

Link back to DTU Orbit

Estimation of Pulses in Ultrasound *B*-Scan Images

Jørgen Arendt Jensen

Abstract—It is shown, based on an expression for the received pressure field in pulsed medical ultrasound systems, that a common one-dimensional pulse can be estimated from individual *A*-lines. An ARMA model is suggested for the pulse, and an estimator based on the prediction error method is derived. The estimator is used on a segment of an *A*-line assuming that the pulse does not change significantly inside the segment. Several examples of use of the estimator on synthetic data and data from a tissue phantom and *in vitro* data measured from a calf's liver are given. They show that a pulse can be estimated, even at moderate signal-to-noise ratios.

I. Introduction

RECENTLY it has been shown that the backscattered pressure field in medical ultrasound *B*-scan images can be described by the equation [1], [2]

$$p_r(\vec{r}_5, t) = v_{pe}(t) \underset{t}{\star} f_m(\vec{r}_1) \underset{r}{\star} h_{pe}(\vec{r}_1, \vec{r}_5, t) \qquad (1)$$

where $\star$ denotes a temporal and $\star$ a spatial convolution. v_{pe} is the pulse-echo wavelet that accounts for the transducer excitation and the electromechanical impulse response during emission and reception of the pulse. f_m accounts for inhomogeneities in the tissue due to density and propagation velocity perturbations, which give rise to the scattered signal. h_{pe} is the modified pulse-echo spatial impulse response that relates the transducer geometry to the spatial extent of the scattered field. Explicitly written, these terms are

$$v_{pe}(t) = \frac{\rho_0}{2} E_m(t) \underset{t}{\star} \frac{\partial v(t)}{\partial t} \qquad (2)$$

$$f_m(\vec{r}_1) = \frac{\Delta \rho(\vec{r}_1)}{\rho_0} - \frac{2 \Delta c(\vec{r}_1)}{c_0} \qquad (3)$$

$$h_{pe}(\vec{r}_1, \vec{r}_5, t) = \frac{1}{c_0^2} \frac{\partial h(\vec{r}_1, \vec{r}_5, t)}{\partial t} \underset{t}{\star} \frac{\partial h(\vec{r}_1, \vec{r}_5, t)}{\partial t}. \qquad (4)$$

$\vec{r}_1$ denotes the position of the scatterer and $\vec{r}_5$ the position of the transducer. c_0 is the propagation velocity, ρ_0 the mean density, and Δc_0, $\Delta \rho$ the corresponding perturbations in the scattering region. $v(t)$ is the transducer exci-

tation and $E_m(t)$ the impulse response when receiving. h is the spatial impulse response for the transducer geometry calculated by the Tupholme–Stepanishen method [3]–[5]. Equation (1) was derived under the assumption of weak scattering due to density and propagation velocity perturbations in the tissue, and absorption and multiple scattering were neglected.

If we assume a homogeneous absorption and we are in the far field then the absorption $A(t, |\vec{r}_1 - \vec{r}_5|)$ can be lumped into v_{pe} to yield an attenuated pulse

$$v_{pea}(t, |\vec{r}_1 - \vec{r}_5|) = v_{pe}(t) \underset{t}{\star} A(t, |\vec{r}_1 - \vec{r}_5|) \qquad (5)$$

that is a function of time and distance.

The attenuated pulse is convolved onto all reflections, and being the common pulse in all *A*-lines, it can thus be estimated from just one *A*-line. The change in this pulse is also the reason for the different appearances of the *B*-scan images of different humans, as attenuation in upper tissue layers changes the pulse that impinges on deeper tissue structures.

A first step in making *B*-scan images with a uniform appearance, by compensating for attenuation, is to estimate the attenuated pulse *in vivo*. This paper describes how to estimate pulses to do this.

Estimation of parameterized pulses from ultrasound *A*-lines has been investigated by a number of authors. Towfig *et al.* [6] used an AR-pulse to discriminate between different tissue types and Kuc and Li [7] used a reduced order AR-model to estimate the center frequency of the pulse spectrum. A model for the attenuation can also be fitted by an AR-model as was done by Shih *et al.* [8]. They also gave a recursive estimator for finding the attenuation. Other parametric models for the attenuation can be given and its parameters estimated as, e.g., in [9].

In this work we will extend the estimation procedure to handle autoregressive moving average (ARMA) models, and we will concentrate on just the estimation of the basic pulse as described above. The parameters can then enter into different other algorithms, e.g., deconvolution [10], [2], attenuation estimation, or reconstruction of the whole pressure field via (1).

The paper proceeds along the following lines. The next section introduces a model for the pulse and describes the general method for estimating the pulse. Section III derives the algorithm and explains how to initialize it. Several examples of its use on both synthetic, phantom, and *in vitro* data from a calf's liver are given in Section IV. The paper is concluded in Section V.

II. Pulse Estimation

A model for the pulse must be chosen before the estimation algorithm can be derived. Several models exist, and can be used [11]. We choose here to use the ARMA model, as it offers considerable flexibility in describing the pulse and as parameter estimators are readily found. It is given by

$$A(q) \, y(k) = C(q) \, e(k) \tag{6}$$

where

$$A(q) = 1 + a_1 q^{-1} + a_2 q^{-2} + \cdots + a_{n_a} q^{-n_a} \tag{7}$$

$$C(q) = 1 + c_1 q^{-1} + c_2 q^{-2} + \cdots + c_{n_c} q^{-n_c} \tag{8}$$

$y(k)$ is the measured output signal and $e(k)$ is the tissue "reflection" signal. $A(q)$ is the autoregressive polynomial of order n_a and $C(q)$ the moving average polynomial of order n_c. We shall refer to this as an ARMA (n_a, n_c) model.

We will, for later use, write the model in a different form. The parameters to be estimated $(a_1 \cdots a_{n_a}$ and $c_1 \cdots c_{n_c})$, are collected in a column vector Θ of order $n_a + n_c$. The different input and output values are organized in a vector $\varphi(k)$ so that

$$y(k) = \varphi^T(k)\Theta + e(k) \tag{9}$$

$$\Theta^T = [a_1, a_2, \cdots, a_{n_a}, c_1, c_2, \cdots, c_{n_c}] \tag{10}$$

$$\varphi^T(k) = [-y(k - 1), -y(k - 2), \cdots,$$
$$-y(k - n_a), e(k - 1), \cdots, e(k - n_c)]. \tag{11}$$

Θ is the unknown parameter vector to be estimated, and $\varphi(k)$ is the regression vector at time k.

This model assumes the parameters to be time independent corresponding to independence of the distance to the transducer. This is not correct according to (5), as the pulse is slowly changing, and thus a new a set of parameters should be estimated for each time instance. We, however, use only a small segment of an A-line in the estimation, where the pulse can be considered stationary.

A. Prediction Error Methods

To find which model is the "best" in the set of models we must be able to assess the quality of the different models.

Ultimately the model describes the observed signal $y(k)$, so one method is to evaluate the prediction capability of the model. That is to say: if all data up to time $k - 1$ are known, what output will the model then predict at time k, $\hat{y}(k|\Theta)$?

For the ARMA-model we have

$$A(q) \, y(k) = C(q) \, e(k)$$
$$\Updownarrow \qquad y(k) = [1 - A(q)] y(k) \tag{12}$$
$$+ [C(q) - 1] e(k) + e(k).$$

Note that the output at time k is written here as a function of the previous input and output plus the current input $e(k)$. As we only have the observation $y(k)$ and estimates of the previous input, the best prediction is

$$\hat{y}(k|\Theta) = [1 - A(q)] y(k) + [C(q) - 1]\hat{e}(k, \Theta) \tag{13}$$

if the mean value of $e(k)$ is zero.

Note here that

$$\hat{y}(k|\Theta) = \varphi^T(k)\Theta. \tag{14}$$

If our model and our estimates of $\hat{e}(k, \Theta)$ are correct, then

$$y(k) - \hat{y}(k|\Theta) = \hat{e}(k, \Theta). \tag{15}$$

The purpose of the parameter estimation is then to minimize the prediction error. A measure of the magnitude of the prediction error is [11]

$$V_N(\Theta, \mathcal{Z}(N)) = \frac{1}{N} \sum_{k=1}^{N} \mathcal{L}(\hat{e}(k, \Theta)) \tag{16}$$

where $\mathcal{L}(\cdot)$ is a scalar-valued positive function and N the number of samples in the segment used for the pulse estimation. $\mathcal{Z}(N)$ denotes the set of all observations, $\{y(1), y(2), \cdots, y(N)\}$.

For this parameter estimation we choose $\mathcal{L}(\cdot)$ to be the quadratic norm, as this is convenient from a computational point of view. Then (16) becomes

$$V_N(\Theta, \mathcal{Z}(N)) = \frac{1}{N} \sum_{k=1}^{N} \frac{1}{2} \hat{e}(k, \Theta) \, \hat{e}(k, \Theta). \tag{17}$$

The parameter estimate then is

$$\hat{\Theta}_N = \operatorname*{Arg\ min}_{\Theta \in D_M} V_N(\Theta, \mathcal{Z}(N)). \tag{18}$$

This means that $\hat{\Theta}_N$ is the minimizing argument of the function $V_N(\Theta, \mathcal{Z}(N))$ under the constraint that the parameters belong to the set of stable models D_M (poles inside the unit circle).

This parameter estimation method is called the prediction error method (PEM) [11], [14]. The prediction error estimation is a maximum likelihood estimator, if the reflection sequence/prediction error is Gaussian [14]. Maximum likelihood estimators have the following properties.

The estimates are consistent, so the estimated parameters tend to the true parameters with probability one, as N (the number of samples) tends to infinity [11].

For the estimator to be consistent the system must be stable, the estimated model must belong to the set of true models, and the data should be informative enough. The last demand is essentially that the input $e(k)$ is "persistently exciting" of order n, when we estimate a model of order n. This means that the spectrum of $e(k)$, $\Phi_E(\omega)$ must differ from zero at more than n points. If

$$\Phi_E(\omega) > 0 \qquad \forall \omega \tag{19}$$

then we call $e(k)$ persistently exciting. This is the case for white noise [11].

The ML-estimator is invariant. This means that

$$\widehat{f(\Theta)} = f(\hat{\Theta}) \qquad (20)$$

which is a consistent estimate of $f(\Theta)$. Thus, the pulse parameters estimated by the algorithm can be used in order ML-algorithms, e.g., attenuation estimation, deconvolution, etc.

These properties are fulfilled when the correct model is used, and the reflection sequence is white and Gaussian as is the case for a speckle signal [15].

Apart from these two properties it can be shown that the estimate is asymptoticlaly efficient. Thus, the variance of the estimate approaches the Cramér–Rao lower bound when N tends to infinity. This is the minimum possible value, so for N large the ML-estimator is the best possible estimator.

III. OFF-LINE PARAMETER ESTIMATION

Our task is to estimate the parameters for the ARMA model of the wavelet. This is a nonlinear optimization problem as $e(k)$ is unknown and cannot be solved in one step. We therefore turn to an iterative search scheme, where the parameters are calculated by

$$\hat{\Theta}_N^{(i+1)} = \hat{\Theta}_N^{(i)} + \alpha g_N^{(i)}. \qquad (21)$$

The parameters are updated for each iteration by adding a search gradient vector, g_N. The iteration number is indicated by i.

A widely used algorithm is the Gauss–Newton algorithm. Here the search gradient is

$$g_N^{(i)} = -[V_N''^{(i)}(\hat{\Theta}_N^{(i)}, \mathcal{Z}(N))]^{-1} V_N'^{(i)}(\hat{\Theta}_N^{(i)}, \mathcal{Z}(N)) \qquad (22)$$

$V_N'^{(i)}(\Theta, \mathcal{Z}(N))$ is the derivative of the criterion with respect to the parameters. $V''^{(i)}(\Theta, \mathcal{Z}(N))$ is the second derivative w.r.t. the parameters, and is also called the Hessian matrix.

If we have a model in which the output is linearly related to the parameters and a quadratic criterion, then (22) will, in one step, lead to the minimum. This is not the case here, but the algorithm leads to the minimum in few steps, when Θ is close to the minimum [11].

The step size, α in (21), is chosen to

$$V_N^{(i+1)}(\hat{\Theta}_N^{(i+1)}, \mathcal{Z}(N)) < V_N^{(i)}(\hat{\Theta}_N^{(i)}, \mathcal{Z}(N)). \qquad (23)$$

Initially α is chosen to be 1 and is reduced by a factor of 2 until (23) is fulfilled or α has been bisected ten times. The algorithm is also stopped when the norm of the gradient search vector falls below a prescribed lower limit.

A. Calculation of Gradients

To find the search gradient g_N, we have to calculate the gradient of the criterion w.r.t. the parameters.

The gradient is [11]

$$\frac{dV_N(\Theta, \mathcal{Z}(N))}{d\Theta_i} = \frac{1}{N} \sum_{k=1}^{N} \frac{d\hat{e}^T(k, \Theta)}{d\Theta_i} \hat{e}(k, \Theta) \qquad (24)$$

$$\frac{d\hat{e}(k, \Theta)}{d\Theta_i} = \frac{d(y(k) - \hat{y}(k|\Theta))}{d\Theta_i} = -\frac{d\hat{y}(k|\Theta)}{d\Theta_i}. \qquad (25)$$

The derivative of the prediction $\hat{y}(k|\Theta)$ w.r.t. Θ is denoted $\psi(k, \Theta)$, so

$$V_N'^{(i)}(\Theta, \mathcal{Z}(N)) = -\frac{1}{N} \sum_{k=1}^{N} \psi^T(k, \Theta) \hat{e}(k, \Theta). \qquad (26)$$

For the ARMA-model (13) we have

$$\hat{y}(k|\Theta) = [1 - A(q)]y(k)$$
$$+ [C(q) - 1](y(k) - \hat{y}(k|\Theta))$$
$$\Updownarrow$$
$$C(q)\,\hat{y}(k|\Theta) = [C(q) - A(q)]y(k). \qquad (27)$$

Then the gradient is

$$C(q) \frac{d\hat{y}(k|\Theta)}{da_j} = -q^{-j}y(k) \qquad (28)$$

$$q^{-j}\hat{y}(k|\Theta) + C(q) \frac{d\hat{y}(k|\Theta)}{dc_j} = q^{-j}y(k)$$
$$\Updownarrow$$
$$C(q) \frac{d\hat{y}(k|\Theta)}{dc_j} = q^{-j}(y(k) - \hat{y}(k|\Theta)) = q^{-j}\hat{e}(k, \Theta). \qquad (29)$$

Comparing to the entries of $\varphi(k)$ in (11) we find that (28) and (29) can be written

$$C(q)\,\psi(k, \Theta) = \varphi(k)$$
$$\Updownarrow \qquad\qquad\qquad\qquad (30)$$
$$\psi(k, \Theta) = \frac{1}{C(q)}\,\varphi(k).$$

So the gradient is calculated by filtering the regression matrix $\varphi(k)$ through the filter $1/C(q)$.

B. Calculation of the Pseudo-Hessian

The Hessian matrix is

$$V_N''^{(i)}(\Theta, \mathcal{Z}(N)) = \frac{d^2 V_N(\Theta, \mathcal{Z}(N))}{d\Theta^2}$$
$$= \frac{dV_N'(\Theta, \mathcal{Z}(N))}{d\Theta}$$
$$= \frac{1}{N} \sum_{k=1}^{N} \psi^T(k, \Theta) \psi(k, \Theta)$$
$$- \frac{1}{N} \sum_{k=1}^{N} \frac{d\psi^T(k, \Theta)}{d\Theta} \hat{e}(k, \Theta). \qquad (31)$$

We choose here to calculate an approximation to the Hessian, whereby the second term in (31) is neglected. If Θ is close to the true value, then $\hat{e}(k, \Theta)$ is nearly white noise and consequently the term is close to zero. Far away from the minimum, when the function values between the current value and the minimum cannot be well approximated by a quadratic function, the effect of the Hessian is not so important [11].

So in the algorithm used, the pseudo-Hessian is defined by

$$V_N''(\Theta, \mathcal{Z}(N)) = \frac{1}{N} \sum_{k=1}^{N} \psi^T(k, \Theta) \, \psi(k, \Theta). \quad (32)$$

C. Initialization

The convergence rate of the algorithm depends on the initial parameter values and the choice of α. When the algorithm is started, some initial values must be chosen. One method is to use a least-squares estimate of Θ and $e(k)$. This can be done by the following algorithm.

Initially consider the ARMA-model

$$A_1(q) \, y(k) = C_1(q) \, e(k) \quad (33)$$

where $e(k)$ is white, and A_1, C_1 are polynomials as defined in (7) and (8). The order of A_1 is set to $n_a + n_c$, and the order of C_1 is set to zero, so

$$y(k) = [1 - A_1(q)] y(k) + e(k). \quad (34)$$

The parameters of A_1 are arranged in a column vector, Θ_{LS1}, of order $n_a + n_c$, and the corresponding output values in a vector φ_1, so (34) can be written

$$y(k) = \varphi_1^T(k) \Theta_{LS1} + e(k). \quad (35)$$

The prediction error is

$$\hat{e}(k, \Theta_{LS1}) = y(k) - \hat{y}(k|\Theta_{LS1}) = y(k) - \varphi_1^T(k) \hat{\Theta}_{LS1}. \quad (36)$$

Our purpose is then to minimize the variance of the prediction error, which is

$$V_N(\Theta_{LS1}, \mathcal{Z}(N))$$
$$= \frac{1}{N} \sum_{k=1}^{N} (y(k) - \varphi_1^T(k) \hat{\Theta}_{LS1})^T (y(k) - \varphi_1^T(k) \hat{\Theta}_{LS1}). \quad (37)$$

As this is a quadratic function of the parameters, the solution is given by the least-squares estimate

$$\hat{\Theta}_{LS1} = \left[\frac{1}{N} \sum_{k=1}^{N} \varphi_1(k) \, \varphi_1^T(k) \right]^{-1} \frac{1}{N} \sum_{k=1}^{N} \varphi_1(k) \, y(k). \quad (38)$$

This can easily be found from (37) by differentiating w.r.t. Θ_{LS1} and setting the result equal to zero.

From this model we can estimate $e(k)$ by

$$\hat{e}(k, \Theta_{LS1}) = y(k) - \varphi_1^T(k) \hat{\Theta}_{LS1}. \quad (39)$$

Then a new model is constructed in which

$$y(k) = [1 - A_2(q)] y(k) + [C_2(q) - 1]\hat{e}(k, \Theta_{LS1})$$
$$+ \hat{e}(k, \Theta_{LS1})$$
$$= \varphi_2^T(k) \hat{\Theta}_{LS2} + \hat{e}(k, \Theta_{LS1}). \quad (40)$$

This is an ARX model (autoregressive with external input), where $\hat{e}(k, \Theta_{LS1})$ is the external input.

The order of A_2 and C_2 are n_a and n_c. Θ_{LS2} is arranged in the same fashion as (10). The parameters can then be calculated by using (38), which results in initial estimates for Θ and $e(k)$ for the iterative search scheme.

D. The Complete Off-Line Algorithm

For easy reference we now give the full algorithm.
1) Fit an AR-model of order $n_a + n_c$ to the data
   Model: $A_1(q) \, y(k) = e(k)$

$$\hat{\Theta}_{LS1} = \left[\frac{1}{N} \sum_{k=1}^{N} \varphi_1(k) \, \varphi_1^T(k) \right]^{-1} \frac{1}{N}$$
$$\cdot \sum_{k=1}^{N} \varphi_1(k) \, y(k).$$

2) Calculate the initial estimate of the prediction error

$$\hat{e}(k, \Theta_{LS1}) = y(k) - \varphi_1^T(k) \hat{\Theta}_{LS1}$$
$$\text{for } k = 1 \text{ to } N.$$

3) Make a least-squares fit to an ARX-model of order n_a and n_c, where the external input is $\hat{e}(k, \Theta_{LS1})$
   Model: $A_2(q) \, y(k) = C_2(q) \, e(k)$

$$\hat{\Theta}_{LS2} = \left[\frac{1}{N} \sum_{k=1}^{N} \varphi_2(k) \, \varphi_2^T(k) \right]^{-1} \frac{1}{N}$$
$$\cdot \sum_{k=1}^{N} \varphi_2(k) \, y(k).$$

This gives the initial parameter estimate for Θ and the prediction error.
4) Initialize the iterative algorithm

$$\hat{e}(k, \Theta) = \hat{e}(k, \Theta_{LS1}) \quad \text{for } k = 1 \text{ to } N$$
$$\hat{\Theta}_N^{(0)} = \hat{\Theta}_{LS2}$$
$$V_N^{(0)}(\Theta, \mathcal{Z}(N)) = \frac{1}{N} \sum_{k=1}^{N} \frac{1}{2} \hat{e}(k, \Theta) \, \hat{e}(k, \Theta).$$

5) Perform the iterative algorithm
   (a) Calculate the gradient

$$\psi(k, \Theta) = \frac{1}{C(q)} \varphi(k)$$
$$V_N'^{(i)}(\Theta, \mathcal{Z}(N)) = -\frac{1}{N} \sum_{k=1}^{N} \psi^T(k, \Theta) \, \hat{e}(k, \Theta).$$

   (b) Calculate the pseudo-Hessian

$$V_N''^{(i)}(\Theta, \mathcal{Z}(N)) = \frac{1}{N} \sum_{k=1}^{N} \psi^T(k, \Theta) \, \psi(k, \Theta)$$
$$\alpha = 1.$$

   (c) Update the parameter vector

$$\hat{\Theta}_N^{(i+1)} = \hat{\Theta}_N^{(i)} + \alpha [V_N''^{(i)}(\Theta, \mathcal{Z}(N))]^{-1}$$
$$\cdot V_N'^{(i)}(\Theta, \mathcal{Z}(N)).$$

   (d) Check the stability of the model:

   Zeros and poles are mirrored into the unit circle.

(e) Calculate the new prediction error

$$\hat{e}(k, \Theta) = y(k) - \varphi^T(k)\Theta_N^{(i+1)}$$

for $k = 1$ to N

$$V_N^{(i+1)}(\Theta, Z(N)) = \frac{1}{N} \sum_{k=1}^{N} \frac{1}{2} \hat{e}(k, \Theta) \hat{e}(k, \Theta).$$

If $V_N^{(i+1)} < V_N^{(i)}$ then go to (a) else $\alpha = \alpha/2$ and go to (c) with the new α until tried ten times. If $\|[V_N''^{(i)}(\Theta, Z(N))]^{-1} V_N'^{(i)}(\Theta, Z(N))\| < \Delta$ then stop. A typical value of Δ is 0.01.

This is the complete off-line algorithm for estimating the wavelet v_{pea}.

E. Convergence Properties

The convergence of maximum likelihood ARMA estimators has been investigated by Åström and Söderström [12]. They showed that a global minimum exits provided that

$$\hat{n}_a \geq n_a \wedge \hat{n}_c \geq n_c \tag{41}$$

where n_a and n_c are the true orders of the polynomials and $\hat{n}_a$, $\hat{n}_c$ the actual ones used. This is under the assumption of no noise in the measured signal and infinitely many data samples.

The influence of using a small number of samples and added noise $n(k)$ has not, to our knowledge, been analyzed analytically in the literature. We are therefore forced to resort to simulations. Ours has indicated that local minima do exist, but that they for signal-to-noise ratio's above 20 to 30 are close to the global minimum. Therefore, it is generally advisable, if possible, to start the iterative search algorithm [step 5)] as close to possible to the true parameters. So the parameters found by steps 1) to 3) should preferably be substituted by good a priori knowledge. How to obtain such knowledge is also explained in Section IV-B.

The disadvantage of using the ARMA model is that the noise in the measured signal is neglected. If noise is present, then the parameters estimated for this model are biased. But if we can write

$$A(q) y(k) = C(q) e(k) + A(q) n(k) \tag{42}$$

where $n(k)$ is white noise, then unbiased parameters will result. The bias depends on the signal-to-noise ratio (SNR). A "large" SNR results in a low bias. As will be clear from the examples, the SNR observed in medical ultrasound is sufficiently high to ensure a good parameter estimation.

The approximation of using the ARMA model rather than a more general model, that accounts for the noise, is fair, if the signal-to-noise ratio is sufficiently "large," and if our algorithm estimates a model that "in the best possible way" approximates the true model. It can be shown under weak conditions (which are fulfilled here) that the estimate from the prediction-error method converges to the best possible approximation of the model

that is included in the set of possible models D_M, when N (the number of samples) tends to infinity. The measure of goodness is the prediction error variance, so formally the convergence result is stated as

$$\hat{\Theta}_N = \text{Arg} \min_{\Theta \in D_M} \left[\frac{1}{N} \sum_{k=1}^{N} \frac{1}{2} \hat{e}(k) \hat{e}(k) \right]$$

w.p. 1 as $N \to \infty$. (43)

For a derivation of this and a further explanation see [11] and [13].

F. Variance of the Estimated Parameters

We have now found that $\hat{\Theta}_N$ converges to the best possible parameters in the set D_M. But we would also like to characterize how $\hat{\Theta}_N$ approaches this model Θ^*, and what the uncertainty of the parameters is. This can be assessed by the parameter variance. We will not derive the expression for the covariance, but merely state the result.

An estimate of the asymptotical covariance of the parameters found by the prediction-error method is

$$\hat{P}_{\Theta_N} = \hat{\lambda}_N \left[\frac{1}{N} \sum_{k=1}^{N} \psi^T(k, \hat{\Theta}_N) \psi(k, \hat{\Theta}_N) \right]^{-1} \tag{44}$$

$$\hat{\lambda}_N = \frac{1}{N} \sum_{k=1}^{N} \hat{e}(k, \hat{\Theta}_N) \hat{e}(k, \hat{\Theta}_N). \tag{45}$$

A derivation and further explanation of the result can be found in [11].

Note here that the covariance estimate can easily be calculated from variables used in the algorithm; the second term in (44) is the inverse pseudo-Hessian matrix.

For N tending to infinity, P_{Θ_N} will approach the Cramér–Rao bound, so the estimate has the best possible asymptotic properties one can hope for [11].

IV. ESTIMATION EXAMPLES

The first step in assessing the performance of the algorithm is to choose a suitable model order. Several experiments made by Jensen [2] have revealed that an ARMA (6, 6) wavelet can adequately fit measured ultrasound pulses for different transducers. Thus we choose to use this model.

Before estimating wavelets from data sampled from a phantom or tissue we want to get an indication of the performance of the algorithm under various noise conditions. This is done by estimating the wavelet from simulated data where the pulse shape is known exactly together with the signal-to-noise ratio (SNR).

A. Wavelet Estimation from Simulated Data

For this use we have the following sixth-order pulse shown in Fig. 1 (——). The ARMA coefficients are

$$A(q) = 1.0000 - 2.3249 q^{-1} + 1.5900 q^{-2} + 1.0265 q^{-3}$$
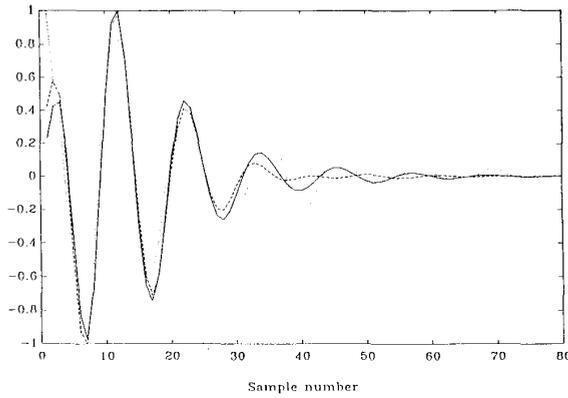$$- 2.2165 q^{-4} + 1.3192 q^{-5} - 0.2665 q^{-6}$$

Fig. 1. Estimated and true wavelet (——), for SNR = 20 (- - -), and for SNR = 4 (· · ·).
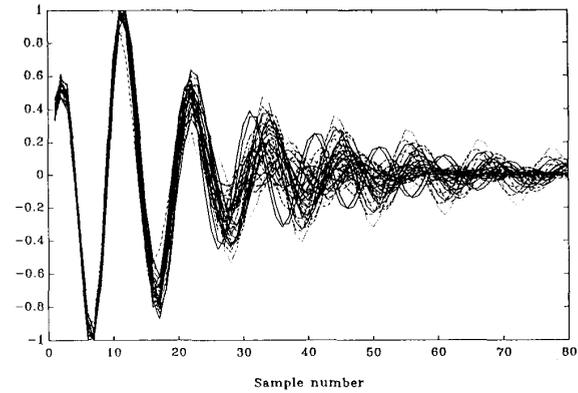

Fig. 2. Wavelets estimated from 50 different realizations of the input and noise signals. SNR = 20.

$$C(q) = 1.0000 - 0.4505 q^{-1} - 0.7837 q^{-2} + 0.0889 q^{-3}$$
$$- 0.3531 q^{-4} - 0.3869 q^{-5} + 0.1731 q^{-6}. \quad (46)$$

This wavelet is convoluted with a zero mean, white, Gaussian signal and then white, Gaussian noise with zero mean is added. The signal-to-noise ratio is defined as

$$\text{SNR} = \sqrt{\frac{E[y(k)^2]}{E[n(k)^2]}} \quad (47)$$

where y is the filtered signal and n the noise. $E[\cdot^2]$ is the covariance.

The first example shows the estimated (- - - -) and true wavelet (——) in Fig. 1, when SNR = 20 and the line contains 500 samples. The solid line is the estimated wavelet, the dashed line is the true wavelet. The estimated wavelet closely resembles the true wavelet.

The estimated parameters and their standard deviations are

$$\hat{A}(q) = 1.000 - 2.1022 q^{-1} + 1.1175 q^{-2} + 1.2707 q^{-3}$$
$$\quad 0 \quad\quad 0.1564 \quad\quad 0.3448 \quad\quad 0.2069$$
$$\quad\quad - 1.9286 q^{-4} + 0.9172 q^{-5} - 0.1137 q^{-6}$$
$$\quad\quad 0.2592 \quad\quad 0.3094 \quad\quad 0.1107$$
$$\hat{C}(q) = 1.000 - 0.7478 q^{-1} - 0.5027 q^{-2} + 0.4022 q^{-3}$$
$$\quad 0 \quad\quad 0.1669 \quad\quad 0.1563 \quad\quad 0.1289$$
$$\quad\quad - 0.5254 q^{-4} + 0.3912 q^{-5} + 0.0747 q^{-6}$$
$$\quad\quad 0.1024 \quad\quad 0.0845 \quad\quad 0.0931.$$
$$\quad (48)$$

It is seen that the estimated parameters equal the true within ± two standard deviations.

To give an indication of the variations due to different input and noise signals, 50 different wavelets have been estimated. The result is shown in Fig. 2, and the mean of the wavelets ± three standard deviations are shown in Fig. 3.
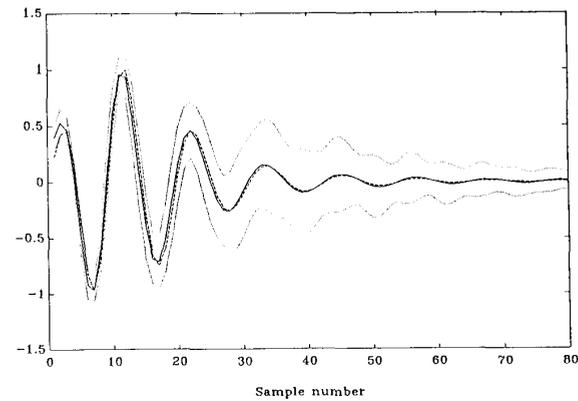

Fig. 3. Mean of the wavelets from Fig. 2, with limits equal to ± three standard deviations. Solid line is the mean of the estimated wavelets.

The mean and variance were calculated by

$$\overline{V}(k) = \frac{1}{N_w} \sum_{i=1}^{N_w} V_i(k) \quad (49)$$

$$\sigma^2(k) = \frac{1}{N_w - 1} \sum_{i=1}^{N_w} (V_i(k) - \overline{V}(k))^2. \quad (50)$$

N_w is the number of wavelets and V_i is the ith wavelet.

Although variations exist, the algorithm always estimates the first two oscillations with a very low standard deviation. The tail of the pulse is more difficult to estimate, and the standard deviation increases. As seen from Fig. 3, the mean of the estimated wavelets is a very close approximation to the true pulse, thus the bias is low even at a fairly moderate signal-to-noise ratio of 20.

However, as mentioned in Section III-E, biased estimates will result when SNR is "low." This is demonstrated in Fig. 1, where the dotted line shows a pulse estimated for SNR equal to 4.

As seen in Fig. 1, the estimated wavelet still approximates the true wavelet especially for the first significant oscillations. It should be noted that this signal-to-noise

ratio is so low that the resulting image would be of very limited clinical value.

If we only consider data where the quantization noise will dominate and assume the input signal is a sinusoid, then for an 8 bit converter SNR is [16]

$$ \mathrm{SNR} = \frac{\dfrac{2^7 \Delta}{2\sqrt{2}}}{\sqrt{\dfrac{\Delta^2}{12}}} = \frac{2^7 \sqrt{6}}{2} = 156 \tag{51} $$

which is quite adequate, even when the full dynamic range of the converter is not used.

B. Wavelets Estimated from Data Measured from a Tissue Phantom

1) Measurement Setup: A Brüel Kjær 8529 transducer with a nominal frequency of 3.5 MHz was used. The transducer is concave with a focal radius of 150 mm and is nonapodized. The radius of the element is 8.1 mm.

The phantom scanned was fabricated by Nuclear Associates (multipurpose tissue/cyst phantom, model 84-317) and contains a substrate which generates a typical backscattered speckle signal. The data were acquired from a region of the phantom by performing a linear scan on the surface. The transducer was moved by an automatic mechanical system, which has a resolution of 0.01 mm [17]. Data were acquired by a LeCroy 9400 sampling oscilloscope. To enhance the signal-to-noise ratio, an averaging over 10 pulse-echo lines, measured at the same position, was performed. The distance between each pulse-echo line is 0.4 mm, and 50 lines were acquired. The distance to the first sample is approximately 9 cm and 10.5 cm to the last sample. The sampling frequency was 25 MHz and 500 samples were acquired.

2) Estimated Wavelets: The mean of the wavelets found by the algorithm along with ± three times the estimated standard deviation is shown in Fig. 4.

A nonattenuated pulse was measured from a plane reflector placed 200 mm from the transducer. A comparison can then be carried out by attenuating this pulse and comparing it to the estimated pulses. Unfortunately no data are given for the attenuation in the phantom. Using 0.5 dB/[MHz · cm] and a distance of 9.75 cm, we get the calculated wavelet also shown in Fig. 4.

Fig. 4 shows that the mean estimated pulse closely approximates the predicted pulse. The most difficult part to model is the tail of the pulse, which is also seen to deviate most from the predicted pulse. Also the standard deviation increases at the tail.

When estimating these pulses no *a priori* information was used. It is quite reasonable to include knowledge measured or estimated previously and use it as a starting point for the wavelet estimation. This has been done in the next experiment. An estimated (shown in Fig. 5) wavelet from the preceding experiment, which approximated the predicted pulse closely, was chosen as the start-
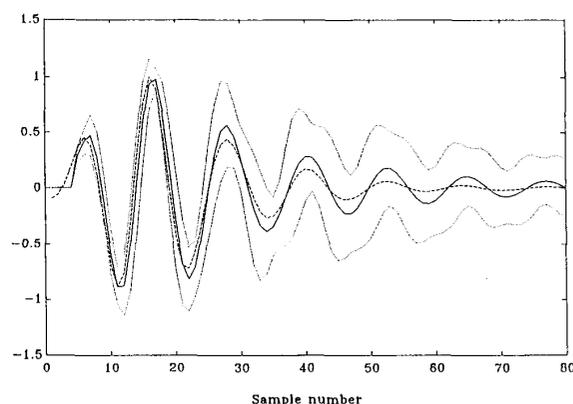

Fig. 4. Mean of estimated wavelets (solid line) from phantom ± three times the standard deviation and the calculated pulse (dashed line).
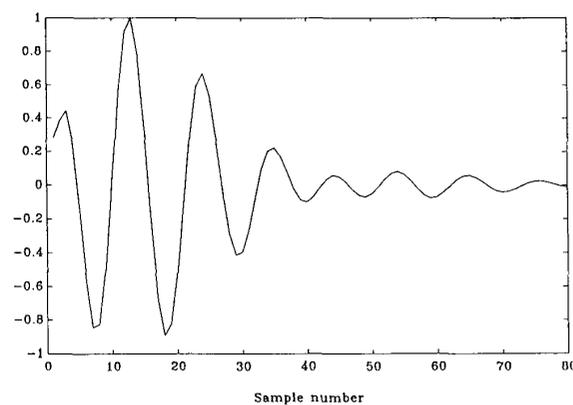

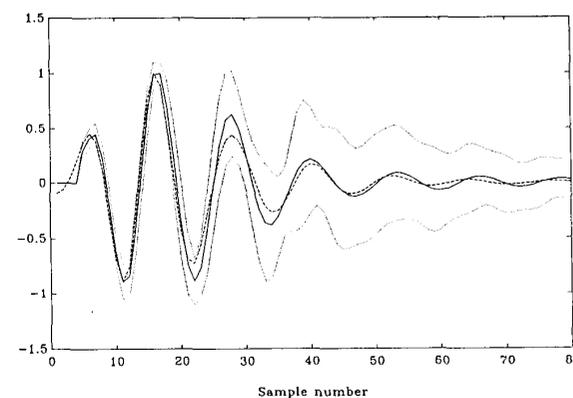
Fig. 5. Wavelet used to initialize the estimator.

Fig. 6. Mean of the estimated wavelets and predicted wavelet for phantom when initialized with the wavelet in Fig. 5.

ing point. Steps 1) to 4) of the algorithm in Section III were then bypassed.

The mean of the estimated wavelets together with the predicted wavelet are shown in Fig. 6. Comparing Fig. 6 to Fig. 4, we see a slight decrease in standard deviation and especially a better prediction of the tail of the pulse.
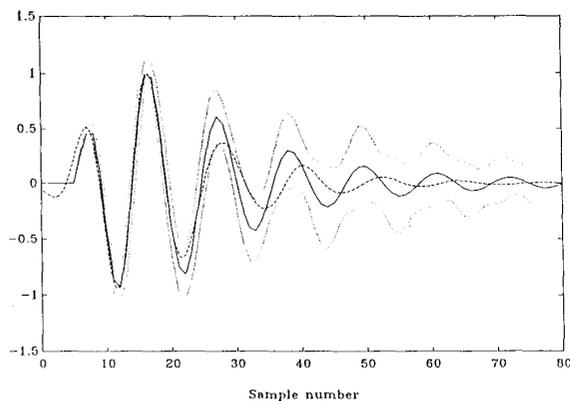
Fig. 7. Mean of estimated wavelets for calf liver *in vitro* ± three standard deviations and predicted wavelet. Solid line is the mean wavelet.
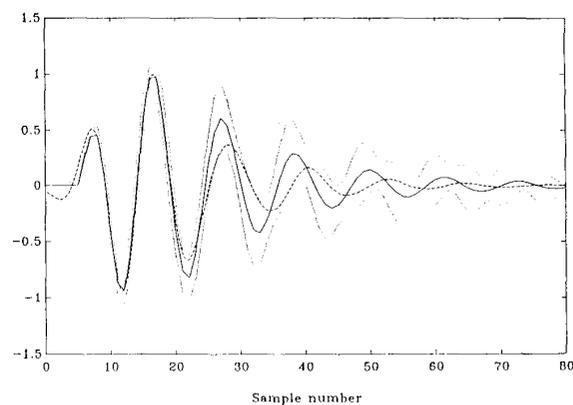

Fig. 8. Mean and predicted wavelet for *in vitro* liver when initialized.

C. Wavelets Estimated from Data Measured from a Calf's Liver

1) Measurement Setup: The data used in this section were measured from a calf's liver submerged in a water bath with a size of 850 × 430 × 500 mm (length × height × width). The liver had been frozen for 5 days and was thawed in a refrigerator for 24 h. After this it was kept in a plastic bag with water and massaged to remove air bubbles. The distance between the liver and the transducer was approximately 6 cm when submerged in the water bath.

Data were taken by performing a linear scan, moving the transducer by the automatic mechanical system. 500 samples were acquired at a sampling frequency of 25 MHz. The first sample was taken at 9 cm, the last at 10.5 cm from the transducer. The LeCroy 9400 digital sampling oscilloscope was used for the acquisition, and each line is the average of 10 lines taken at the same position. 50 pulse-echo lines were acquired. The distance between the lines is 0.2 mm.

2) Estimated Wavelets: The mean of the estimated 50 wavelets ± three standard deviations along with the predicted wavelet is shown in Fig. 7.

The predicted wavelet was calculated by using the wavelet measured from the planar reflector and correcting it by an attenuation of 0.5 dB/[MHz · cm] for a distance of 3.75 cm, as the distance to the start of the liver was 6 cm.

As in Section IV-B, the estimate can be slightly improved by using *a priori* information. The result is shown in Fig. 8. We note here that the estimates obey the same pattern as found in Sections IV-A and -B. The first main oscillations are well estimated, and the variance increases at the tail of the pulse. The estimated mean wavelet is slightly improved, although the improvement is less pronounced than in Section IV-A.

It should be noted that although we compare it to a predicted wavelet, this wavelet is not the true wavelet. Our predicted wavelet is also encumbered with uncertainty, as

the attenuation assumed is uncertain, making the comparison in Figs. 7 and 8 difficult.

V. SUMMARY

It was derived, from a description of the backscattered pressure field, that the scattered signal is convolved with a pulse common to all reflections. This pulse can include the dispersive attenuation in tissue and explain the varying appearance of ultrasound images for different humans.

A first step in compensating for this variability is to estimate the basic pulse. An ARMA model was suggested for the pulse and an estimator was derived based on the prediction error method. The pulse is estimated for a segment of an A-line.

Experiments performed on synthetic data show that the algorithm estimates the wavelet even at low signal-to-noise ratios accurately and consistently. A signal-to-noise ratio of 20 is sufficient to get a precise estimate and the wavelet can be found even at lower ratios, however, with less accuracy.

Experiments performed on data from a tissue phantom and a calf's liver have revealed that the wavelet can also be determined here. Especially the first main oscillations in the pulse are estimated with good accuracy.

The estimator derived here assumes a fixed pulse in the segment used for the estimation. The dispersive attenuation, however, gradually changes the pulse. Therefore, it would be more appropriate to estimate a new pulse for each sampling instance. Algorithms to do this have been derived [11], [14], [2] and we are currently studying the performance of these.

Further research is also underway to find the performance of the estimator for *in vivo* data. This will be reported in a later paper.

REFERENCES

[1] J. A. Jensen, "A model for the propagation and scattering of ultrasound in tissue," *J. Acoust. Soc. Amer.*, vol. 89, no. 1, pp. 182–191, 1991.
[2] ——, "Medical ultrasound imaging, an estimation based approach," Ph.D. dissertation, Electron. Inst., Tech. Univ. Denmark, Sept. 1988.

[3] G. E. Tupholme, "Generation of acoustic pulses by baffled plane pistons," *Mathematika*, vol. 16, pp. 209-224, 1969.

[4] P. R. Stepanishen, "The time-dependent force and radiation impedance on a piston in a rigid infinite planar baffle," *J. Acoust. Soc. Amer.*, vol. 49, no. 3, pp. 841-849, 1971A.

[5] ——, "Transient radiation from pistons in a infinite planar baffle," *J. Acoust. Soc. Amer.*, vol. 49, pp. 1627-1638, 1971B.

[6] F. Towfig, C. W. Barnes, and E. J. Pisa, "Tissue classification based on autoregressive models for ultrasound pulse echo data," *Acta Electron.*, vol. 26, pp. 95-110, 1984.

[7] R. Kuc and H. Li, "Reduced order autoregressive modeling for center-frequency estimation," *Ultrason. Imaging*, vol. 7, pp. 244-251, 1985.

[8] L. Y. Shih, C. W. Barnes, and L. A. Ferrari, "Estimation of attenuation coefficient for ultrasonic tissue characterization using time-varying state-space model," *Ultrason. Imaging*, vol. 10, pp. 90-109, 1988.

[9] G. Salmonsson and B. Löfström, "Analysis of a system for ultrasonic imaging of attenuation and texture in soft tissue," *Ultrason. Imaging*, vol. 7, pp. 225-243, 1985.

[10] M. Fatemi and A. C. Kak, "Ultrasonic B-scan imaging: Theory of image formation and a technique for restoration," *Ultrason. Imaging*, vol. 2, pp. 1-47, 1980.

[11] L. Ljung, *System Identification, Theory for the User*. Englewood Cliffs, NJ: Prentice-Hall, 1987.

[12] K. J. Åström and T. Söderström, "Uniqueness of the maximum likelihood estimates of the parameters of an ARMA model," *IEEE Trans. Automat. Contr.*, vol. AC-19, no. 6, pp. 769-773, 1974.

[13] L. Ljung, "Convergence analysis of parametric identification methods," *IEEE Trans. Automat. Contr.*, vol. AC-23, no. 5, pp. 770-783, 1978.

[14] L. Ljung and T. Söderström, *Theory and Practice of Recursive Identification*. Cambridge, MA: The M.I.T. Press, 1983.

[15] R. F. Wagner, S. W. Smith, J. M. Sandrick, and H. Lopez, "Statistics of speckle in ultrasound B-scans," *IEEE Trans. Sonico. Ultrason.*, vol. 30, no. 3, pp. 156-163, May 1983.

[16] A. V. Oppenheim and R. W. Schafer, *Digital Signal Processing*. Englewood Cliffs, NJ: Prentice-Hall, 1975.

[17] J. A. Jensen and B. Stage, "A high precision transducer measurement system," Electron. Inst., Tech. Univ. Denmark, Rep. C.2, 1989.